



**HAL**  
open science

## Analysis of coherent surface wave dispersion and attenuation for non-destructive testing of concrete

Mathieu Chekroun, Loïc Le Marrec, Odile Abraham, Olivier Durand,  
Géraldine Villain

► **To cite this version:**

Mathieu Chekroun, Loïc Le Marrec, Odile Abraham, Olivier Durand, Géraldine Villain. Analysis of coherent surface wave dispersion and attenuation for non-destructive testing of concrete. *Ultrasonics*, 2009, 49 (8), pp 743-751. 10.1016/j.ultras.2009.05.006 . hal-00436273

**HAL Id: hal-00436273**

**<https://hal.science/hal-00436273>**

Submitted on 25 Sep 2018

**HAL** is a multi-disciplinary open access archive for the deposit and dissemination of scientific research documents, whether they are published or not. The documents may come from teaching and research institutions in France or abroad, or from public or private research centers.

L'archive ouverte pluridisciplinaire **HAL**, est destinée au dépôt et à la diffusion de documents scientifiques de niveau recherche, publiés ou non, émanant des établissements d'enseignement et de recherche français ou étrangers, des laboratoires publics ou privés.

# Analysis of coherent surface wave dispersion and attenuation for non-destructive testing of concrete

M. Chekroun<sup>a,b,\*</sup>, L. Le Marrec<sup>c</sup>, O. Abraham<sup>a</sup>, O. Durand<sup>a</sup>, G. Villain<sup>a</sup>

<sup>a</sup>Laboratoire Central des Ponts et Chaussées (LCPC) - Nantes, France

<sup>b</sup>Électricité de France (EDF R&D) - Chatou, France

<sup>c</sup>Institut de Recherche Mathématique de Rennes (IRMAR) - Rennes, France

---

## Abstract

Rayleigh waves measurements are used to characterise cover concrete and mortar in the frequency range 60-180 kHz. At these frequencies, the wavelength is comparable to the size of the aggregates, and waves propagate in a multiple scattering regime. Acquired signals are then difficult to interpret due to an important *incoherent* part. The method proposed here is the study of the *coherent* waves, obtained by averaging signals over several configurations of disorder. *Coherent* waves give information on an equivalent homogeneous medium. To acquire a large amount of measurements with accuracy, an optimised piezoelectric source is used with a laser interferometer for reception. Adapted signal processing techniques are presented to evaluate the coherent phase and group velocities and also the coherent attenuation parameter. The sensitivity of these three parameters with the properties of concrete is discussed, as well as the necessity to use coherent waves to obtain accurate results.

*Key words:* concrete, Rayleigh waves, ultrasounds, laser interferometer, scattering, effective medium, dispersion, attenuation, signal processing

---

## 1. Introduction

On-site non-destructive evaluation of concrete is a major issue for monitoring the durability of civil engineering structures. Concrete structures are subjected to aggressive attacks from the outside (water, chlorides, weathering variations, ...) which may minimise their durability. In particular, near surface concrete is directly in contact with these aggressive attacks. This cover concrete thickness is 30-50 mm and it essentially protects the steel reinforcing bars from corrosion [1], which can induce macro-cracks due to the expansion of the steel. An early diagnostic of the pathologies of cover concrete may prevent expensive repairs.

Among all non-destructive testing methods available for concrete [2], the use of ultrasonic waves is of great interest to evaluate mechanical properties. Velocity and attenuation of such waves can be used to determine the viscoelastic properties (such as Young Modulus, Poisson ratio, or Lamé coefficients), and also to characterise micro-structural properties of materials (porosity, grain size, micro-cracks, ...). The first method employed for over 50 years was the

---

\*Corresponding author.

Email addresses: [mathieu.chekroun@lcpc.fr](mailto:mathieu.chekroun@lcpc.fr) (M. Chekroun)

23 ultrasonic pulse velocity [2, 3, 4], consisting in measuring the time taken by an ultrasonic pulse  
24 to travel through a concrete sample.

25 However, precise measurements and their interpretations are difficult due to the inherent  
26 strongly heterogeneous nature of concrete. Concrete is basically composed of a mix of cement,  
27 sand, water and coarse aggregates. Sand are small particles with a mean diameter below 4 mm,  
28 while aggregates are the largest particles with dimensions varying from a few millimetres up  
29 to 20 mm or larger. Mortar can be distinguished from concrete because it contains only the  
30 small particles (sand, cement, water) without the coarser aggregates. Mortar and concrete also  
31 contains pores and capillaries, with sizes from about  $10^{-6}$  mm to a few millimetres. These pores  
32 may be filled with air or water. Porosity of these cement paste materials can be directly linked  
33 with the water to cement ratio by mass ( $w/c$ ) of the mix proportions of the concrete. All these  
34 heterogeneities, of various size range, strongly affects the propagation of ultrasonic waves, their  
35 influence depending on the frequencies used.

36 In the past 10 years, with the improvements in transducer design, computing and signal  
37 processing, several experimental studies, using through-transmission ultrasonic measurements,  
38 with compression or shear waves, have been carried out on different cement paste materials:  
39 cement, mortar or concrete.

40 On a pure cement matrix, measurements above 500 kHz show an increase of the attenuation  
41 factor when 10% of entrained air voids of 1 mm diameter are present [5]. Measurements on  
42 fresh mortar [6] shows that the influence of similar air voids is negligible below 500 kHz. In  
43 the same experiment, it is shown that the influence of sand particles with a 1-4 mm diameter on  
44 the attenuation factor is only noticeable above 500 kHz. Influence of air voids, represented by  
45 expanded polystyrene spheres of 2 mm diameter, in a cement-paste matrix with small aggregates  
46 (4-8 mm), is presented in [7]. All of these studies show that the influence of air voids and small  
47 sand particles on the velocity or the attenuation factor at low frequencies (below 500 kHz) is very  
48 low.

49 Influence of grain size (sand and aggregates) was particularly underlined in [8] and [9], com-  
50 paring the frequency dependence of the attenuation and pulse velocity of compression waves on  
51 cement, fine mortar, coarse mortar and concrete, over the range 50-1000 kHz. In particular, only  
52 coarse aggregates with a diameter greater than 5 mm have a significant influence below 200 kHz.  
53 The influence of grain size is clearly visible on the attenuation of the waves while the  $w/c$  ratio  
54 mainly affects the pulse velocity.

55 All these studies [5, 6, 7, 8, 9] consider through-transmission measurements. Another way to  
56 characterise concrete or mortar is to use surface measurements. Rayleigh waves are well adapted  
57 to the characterisation of near surface deterioration of concrete, as their penetration depth is  
58 close to the wavelength. Thus they are suitable to provide information about the first centimetres  
59 of the concrete. Another advantage of surface waves is that they are more convenient for on-  
60 site measurements than through-transmission measurements, since most concrete structures are  
61 accessible only on one side.

62 Young modulus and Poisson ratio have been extracted from low frequency Rayleigh mea-  
63 surements (50 kHz) in [10], using simple compression waves transducers. Wedge transducers  
64 were used in [11, 13] to optimise the generation of Rayleigh waves on mortar, showing the high  
65 sensitivity of these waves with the cover degradation of the samples for frequencies higher than  
66 50 kHz. The potential use of lasers for generation and detection of Rayleigh waves on concrete  
67 is presented in [14] and applied in [15, 16] on mortar slabs, allowing non-contact measurements  
68 over the range 200-1000 kHz. In this frequency range, it is shown that the scattering by small  
69 particles ( $< 5\text{ mm}$ ) does not dominate attenuation compared to the absorption losses. A third

70 way to generate Rayleigh waves is the use of a pencil lead break in [17, 18], which produces a  
71 point-like source with a bandwidth 0-200 kHz, but with very low energy : piezoelectric transduc-  
72 ers were used for the reception at short distance away from the source. The medium was mortar  
73 with small thin vinyl plate inclusions, simulating small cracks in cement. The study show that  
74 Rayleigh waves are more sensitive to this kind of inclusions than compression waves, and that  
75 the effect of the shape of these inclusions is important.

76 Another interest of Rayleigh waves is their ability to evaluate properties varying with depth,  
77 especially in the case of layered media, for example a damaged layer over a sound material. This  
78 approach is classically used in geophysics. Attempts of using this property of Rayleigh waves  
79 on mortar have been envisaged in [19], and on concrete in [20].

80 All studies show the influence of the heterogeneities of mortar or concrete in different fre-  
81 quency range. The objective of this paper is the evaluation of cover concrete with Rayleigh  
82 waves. The depth of penetration of Rayleigh waves is close to the wavelength, therefore, to in-  
83 vestigate the three first centimetres of concrete, frequencies over the range 50-200 kHz will be  
84 used, providing wavelength from about 10 to 50 mm. In this frequency range, the effect of pores  
85 and small particles ( $< 5\text{ mm}$ ) on the attenuation and velocity is negligible compared to absorption  
86 losses, but the coarser aggregates will interact strongly with the waves.

87 The first part of the paper introduces the process needed to focus on global properties of  
88 concrete. Then experimental configuration will be described. In the third chapter particular  
89 attention will be drawn to the acquisition setup, allowing the use of very precise methods to  
90 evaluate phase and group velocity dispersion curves and attenuation factor. The last chapter give  
91 results in terms of field properties for various concrete and mortar. All the following is written  
92 trying to determine some mechanical and micro-structural signatures from the field properties.

## 93 2. Homogeneous effective medium

94 Concrete can be considered as a random distribution of scatterers (aggregates) of different  
95 nature, shape and size in a cement matrix. Waves propagating in such media with a wavelength  
96 comparable to the size of scatterers will propagate in a multiple scattering regime. As a result,  
97 the measured signals will be composed of a coherent part independent to the specific position  
98 of scatterers [21], and also of an important incoherent part specific to the given configuration of  
99 heterogeneities encountered.

100 Then it is possible to take into account an aspect of the randomness by considering the aver-  
101 age value of the measurements over a statistical ensemble of collections of scatterers. This notion  
102 was introduced by Foldy in 1945 [22]. During the propagation, a part of the energy is transfered  
103 from the coherent part into the incoherent part due to multiple scattering. When performing the  
104 ensemble average the incoherent part is eliminated, and only the coherent part survives. The  
105 energy transfered to the incoherent part is lost and this induce an additional attenuation of the co-  
106 herent part. This field can be interpreted as the field propagating in an equivalent homogeneous  
107 medium also called effective medium.

108 The incoherent part doesn't resists to the averaging of disorder. It is composed of all the late  
109 arrivals of wave trains multiply scattered by the heterogeneities and is sometimes called "coda".  
110 This "coda" is often considered as noise, but still contains exploitable information [23, 24]. This  
111 paper will only focus on the coherent part of the signals.

112 In order to evaluate the mechanical properties of concrete, studying a single configuration  
113 of disorder will lead to inaccurate results. Indeed, the signal containing an important incoherent

114 part, the results will mainly depend on the specific configuration of aggregates at the given point,  
 115 and not on the general properties of the concrete. The evaluation of the coherent field allows  
 116 to avoid this problem. In this case the phase velocity, group velocity and attenuation factor of  
 117 the field will give information on the effective medium what can be interpreted as the average  
 118 mechanical properties of the concrete.

119 It is then essential to perform measurements on numerous equivalent configurations of disorder,  
 120 i.e. at different positions on the tested sample of concrete, using the same source and the  
 121 same receiver and at the same distance of propagation. This approach have been used on concrete  
 122 by [7] with through transmission measurements and [17, 18] with surface waves. [7] used  
 123 9 configurations of disorder, and [17, 18] used about 30 equivalent configurations to obtain the  
 124 coherent part.

### 125 3. Experimental procedure

#### 126 3.1. Concrete slabs

127 The measurements are carried out on concrete slabs of  $60\text{ cm} \times 60\text{ cm} \times 12\text{ cm}$ . There are two  
 128 different series of concrete with different  $w/c$  and a maximum grain size ( $D_{max} = 20\text{ mm}$ ). Two  
 129 series of mortar ( $D_{max} = 4\text{ mm}$ ) are made with the same  $w/c$  than the concretes. The characteristics  
 130 of each series are summarised in table 1, and the granulometric curves are presented in  
 131 Fig. 1. Each series is composed of 5 slabs.

	$w/c = 0.35$	$w/c = 0.65$
$D_{max} = 20\text{ mm}$	B1	B2
$D_{max} = 4\text{ mm}$	M1	M2

Table 1: Characteristics of each series of concrete and mortar.

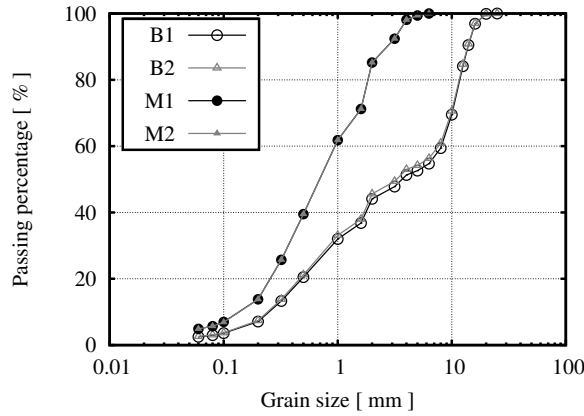


Figure 1: Granulometric curves of the concrete and mortar specimens.

132 The water content of concretes or mortars have been shown to have a significant influence on  
 133 the propagation of ultrasound [12]. In order to guarantee a constant water content of the concrete  
 134 slabs, they are stored immersed in water with additional lime. The water content ratio of the

135 slabs is then very close to 100%. The slabs are taken out of the water only during the ultrasonic  
 136 measurements (a few hours). When the measurements were performed, the slabs had an age  
 137 between 6 and 10 months. At this age, the mechanical properties of concrete are assumed to be  
 138 stabilised.

### 139 3.2. Experimental setup

140 The experimental setup is similar to multi-station acquisition commonly used in geophysics  
 141 : a source emits a wavefield and the measurements are performed with a linear array of receivers  
 142 away from the source. In the present case, the source will be repetitive and the receiver will be  
 143 moved along a line to reproduce an array of reception points.

144 Rayleigh waves are generated with a piezoelectric transducer (Imasonic). The transducer  
 145 emits a compression wave and is equipped with a wedge to allow an incidence of the emitted  
 146 wave with the concrete slab at an angle favouring the conversion to Rayleigh waves [13]. The  
 147 wedge is coupled with the concrete with Gel D (Sofranel) over a thin scotch-tape. The scotch-  
 148 tape avoids the gel to penetrate into the concrete, and makes the manual positioning of the wedge  
 149 easier. The center frequency of the transducer is 120 kHz. It is excited with a Ricker wavelet  
 150 amplified by a Ritec Gated RF amplifier. The bandwidth at -20 dB of the emitted Rayleigh waves  
 151 ranges from 50 kHz to 200 kHz.

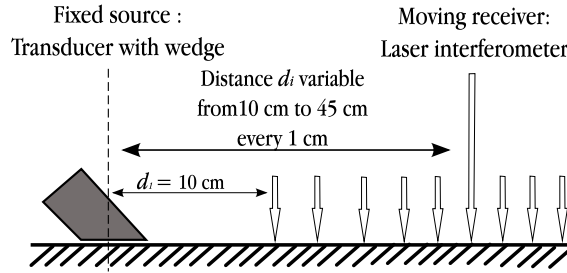


Figure 2: Experimental setup

152 The reception is performed with a laser interferometer (Tempo by BossaNova Tech.). It  
 153 allows non contact acquisition of the normal displacement of the surface of the concrete slab. The  
 154 beam diameter of the laser is around  $50 \mu\text{m}$ , so the measurements are point-like. A reflecting tape  
 155 on the concrete enhance the quality of the signals [14]. The reflective tape is carefully positioned  
 156 on the concrete surface to ensure that no voids are present. The laser interferometer is mounted  
 157 on an automatic measurement bench. The laser is moved along a line in front of the transducer  
 158 to have measurements at different distances of propagation  $d_i$  between 10 cm and 45 cm. The  
 159 first reception point is taken at  $d_1 = 10$  cm from the source to avoid near offset effects. A signal  
 160 is acquired every  $\delta d = 10$  mm, so that the whole profile is composed of 36 signals. Figure 2  
 161 presents the experimental setup. To reduce the signal to noise ratio, each signal is time-averaged  
 162 over 256 acquisitions at each reception point.

163 In order to have different configurations of disorder to evaluate the coherent field, 9 parallel  
 164 profiles, separated of  $L = 40$  mm, are acquired on both sides of the slabs.  $L$  was chosen so that  
 165  $L > D_{max}$  and  $L > \lambda_{max}/2$  to ensure that profiles are not correlated. As there are 5 slabs for  
 166 each series, we acquire a data-set of 90 different multi-station profiles for each concrete series  
 167 B1 and B2. Only 36 profiles were acquired for mortar series M1 and M2 as the heterogeneities

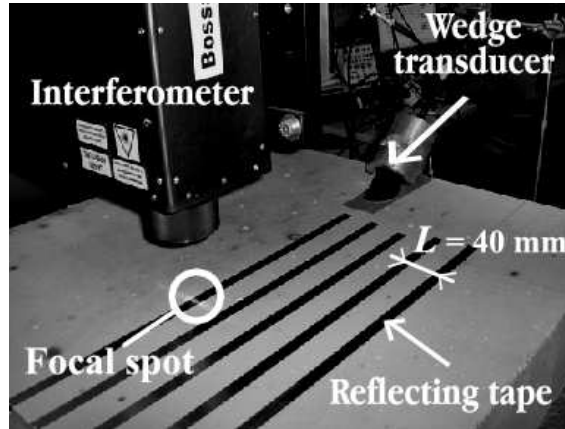


Figure 3: Acquiring parallel profiles to obtain different configurations of disorder

168 of mortar are too small to generate an important incoherent part for the frequencies considered.  
 169 Figure 3 shows a picture of the setup, with the wedge transducer and the laser interferometer.  
 170 The reflecting tapes shows the positions of different acquisition profiles.

#### 171 4. Coherent field

##### 172 4.1. Preprocessing

173 Before evaluating the dispersion and attenuation curves, some pre-processing have to be  
 174 undergone to eliminate artifacts due to the experimental setup.

175 For each profile measured, the source transducer was placed by hand, and the focus of the  
 176 laser beam was adjusted. The whole 36 signals of the profile were automatically acquired with  
 177 the same adjustments, so that the amplitudes of these signals are comparable one from the others.  
 178 On the contrary, from one profile to another the adjustments change and the amplitudes  
 179 are not fully comparable. For example Fig. 4 presents the maximum amplitude of the measured  
 180 displacement for each profile of the series B2 at the offset  $d_1 = 10 \text{ cm}$ . The average maximum  
 181 amplitude is about  $100 \text{ \AA}$  but the variation is very important, up to  $750 \text{ \AA}$ . This effect is corrected  
 182 by normalising each profile by the maximum amplitude of its first signal (at offset  $d_1 = 10 \text{ cm}$ ).  
 183 Doing so, the relative amplitude variation inside a given profile remains the same, but all dif-  
 184 ferent profiles become comparable. The absolute displacement is not needed by the following  
 185 signal processing methods, as they only use relative variations of phase or amplitude along the  
 186 propagation path.

187 Another effect of the hand positioning of the source transducer is that the transducer can-  
 188 not be positioned exactly at the same distance from the first reception point. The difference, a  
 189 few millimetres, induce short time-lags between the signals from a profile to the others. These  
 190 time-lags are evaluated doing cross-correlation between the first signals of each profile, and the  
 191 correction is applied on all the signals of the profile.

192 Figure 5 presents two single seismograms for two given profiles on a concrete slab on the  
 193 series B2. All signals present an important incoherent part that fluctuates from one seismogram  
 194 to the other. Some of these individual signals are presented in gray on figure 6, along with the  
 195 coherent signal.

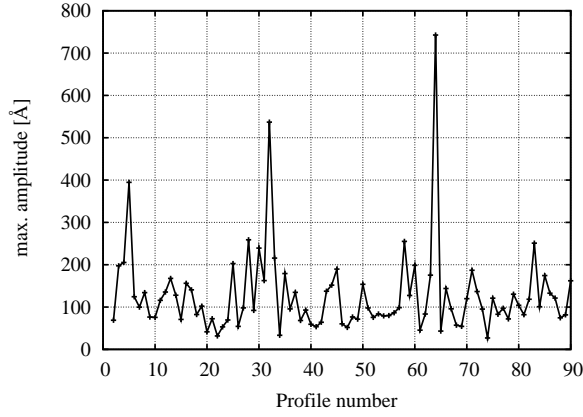


Figure 4: Maximum amplitude of displacement in Å for each signal of series B2 at the offset  $d = 10$  cm.

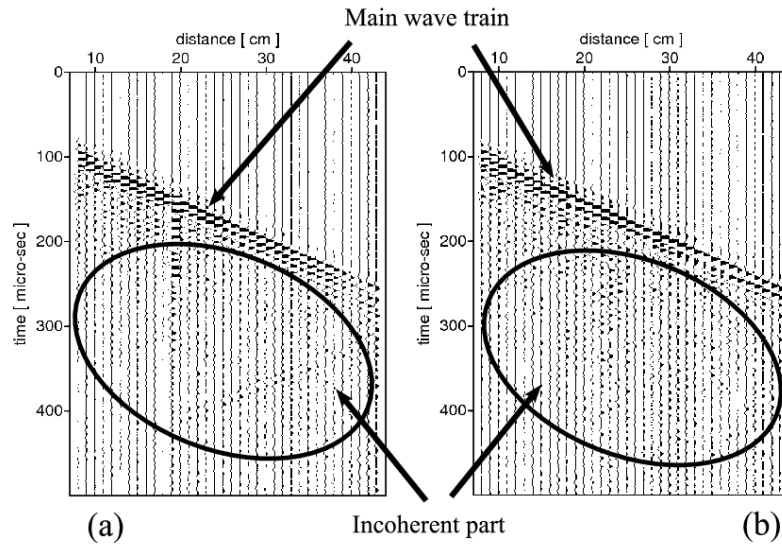


Figure 5: Comparison between two given profiles measurements for series B2.

196 The coherent field for each series is obtained by spatially averaging the different equivalent  
 197 configurations of disorder (90 configurations for concretes B1 and B2, and 36 configurations  
 198 for mortars M1 and M2). In elastic media the amplitude of surface waves decreases with the  
 199 distance of propagation  $d$  as  $1/\sqrt{d}$  due to geometrical spreading in the case of a point source or  
 200 in the axis perpendicular to a line source. This approximation in  $1/\sqrt{d}$  is still valid in the axis of  
 201 our transducers. This decrease is contained in the attenuation measurements and is corrected on  
 202 this coherent field to focus on the material properties (multiple scattering by heterogeneities and  
 203 viscoelasticity effects).

204 The coherent field for series B2 is presented in figure 7-(a), incoherent contributions to the

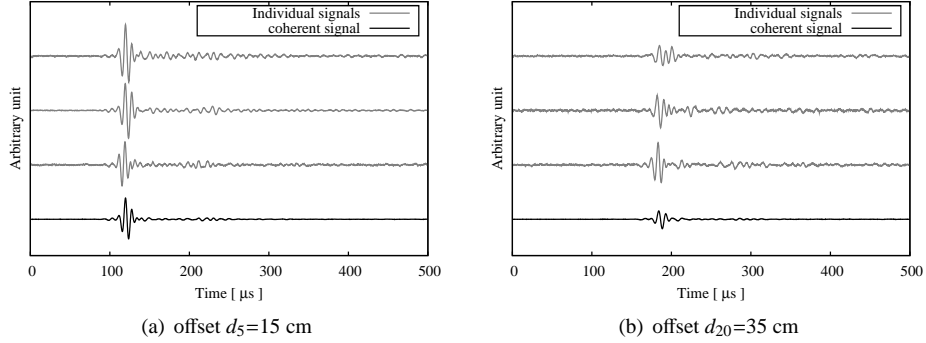


Figure 6: Visualisation of some individual signals, and the corresponding coherent field for B2.

205 field are no longer visible on the seismogram and two main wave trains can be noticed. The  
 206 first one is the most important and corresponds to the coherent Rayleigh wave. The second one  
 207 is parallel to the first one : it is a wave travelling in the same direction and with approximately  
 208 the same velocity as the main wave train. This second wave train corresponds to a reflection  
 209 of the wave emitted by the transducer inside the wedge. To eliminate artifacts induced by this  
 210 reflection, the main wave train is windowed with a flat top Hann window. The width of the  
 211 window was kept constant for all distances of propagation. The resulting coherent seismogram  
 212 for B2 is presented on figure 7-(b).

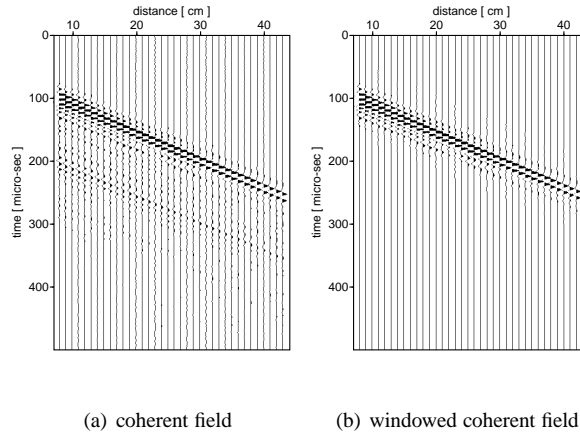


Figure 7: Averaged profile over 90 configurations for B2. (a) non windowed coherent field, (b) coherent field windowed around the main wave train.

#### 213 4.2. Amplitude spectrum

214 The amplitude spectrum provides useful information about the propagation. The major part  
 215 of all the processing to evaluate phase and group velocity and the attenuation factor will be done  
 216 in the frequency domain.

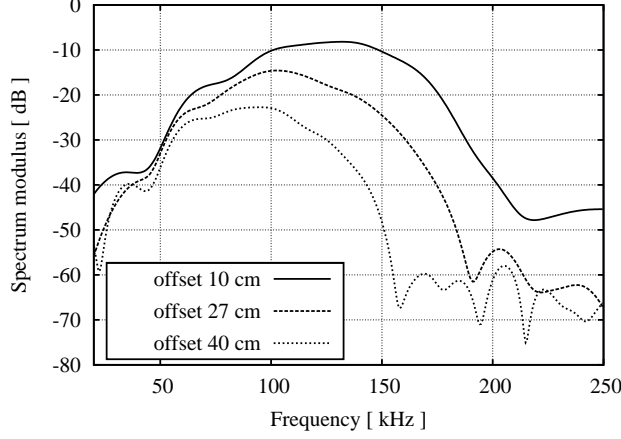


Figure 8: Spectrum modulus of the windowed coherent field at different distances of propagation for series B2.

217 Figure 8 presents an example of the spectrum modulus of the windowed coherent field for  
 218 the concrete series B2, at different distances of propagation; the first reception point at 10 cm, in  
 219 the middle of the profile at 27 cm, and the last reception point at 45 cm. The transducer center  
 220 frequency is 120 kHz, and its bandwidth ranges from 60 kHz to 180 kHz. Figure 8 shows that the  
 221 higher frequencies are more attenuated as the distance of propagation increases; the last reception  
 222 points will not be suitable to evaluate the effective parameters for the higher frequencies.

## 223 5. Signal processing methods

### 224 5.1. Phase velocity

225 The coherent phase velocity  $v_\varphi(\omega)$  is computed using the  $p-\omega$  transform. This method  
 226 is commonly used to study the dispersion of surface waves in geophysics [26, 27, 28, 36]. It  
 227 consists in transforming the entire data wave field into the slowness-frequency domain, where  
 228  $p$  represents the slowness of the waves ( $p = 1/v_\varphi$ ) and  $\omega$  the angular frequency. It was first  
 229 described by McMechan and Yedlin (1981) in the time domain [25]. Mokhtar (1981) proposed  
 230 another formulation of this method entirely in the frequency domain which is used here [26].

231 In the case of media with a single mode of propagation of the waves with the slowness  $p_0(\omega)$ ,  
 232 the Fourier transform over time of the coherent field  $s(\omega, d_i)$  at the angular frequency  $\omega$  and at  
 233 the distance of propagation  $d_i$  can be written as:

$$s(\omega, d_i) = A(\omega, d_i)e^{-i\omega p_0(\omega)d_i}, \quad (1)$$

234 where  $A(\omega, d_i)$  is the amplitude spectrum at  $d_i$ . The  $p-\omega$  stack  $\hat{s}(\omega, p)$  is

$$\hat{s}(\omega, p) = \sum_{i=1}^N A(\omega, d_i)e^{i\omega(p-p_0(\omega))d_i}. \quad (2)$$

235 The computation of  $\hat{s}(\omega, p)$  is performed for several values of  $p$ . Given  $\omega$ , the maximum of the  
 236 modulus  $|\hat{s}(\omega, p)|$  is reached for  $p = p_0(\omega)$ ; the  $|\hat{s}(\omega, p)|$  map is plotted as a 2-D function of  $p$  and  
 237  $\omega$  and the maximum locus is extracted for each frequency.

238 Some problems of aliasing and limited resolution may be encountered as in any spectral  
 239 analysis of discrete data. All these artifacts were described by Forbriger (2003) [27]. Aliasing  
 240 occurs when the distance  $\delta d$  between two reception points is too large compared to the shortest  
 241 wavelength considered, while resolution is limited by the total length of the acquisition setup  
 242 (i.e. the distance between the first and the last receiver). In general, the longest wavelength  
 243 accessible (corresponding to the lowest desired frequency) is assumed to be shorter than 40-50%  
 244 of the total length of the acquisition setup. If this setup is too short, the estimated phase velocity  
 245 for the lower frequencies will be inaccurate.

246 Experimental setup presented in Sec. 3.2 was designed to take account of all these artifacts  
 247 and to provide accurate measurements in the bandwidth 60kHz-180kHz. For the lowest frequen-  
 248 cies, all the reception points will be used to evaluate  $v_\varphi(\omega)$ , to have an acquisition setup long  
 249 enough. For the highest frequencies, only the reception points containing enough energy at these  
 250 frequencies compared to the noise level will be used, as seen in Fig. 8.

## 251 5.2. Group velocity

252 It is theoretically possible to deduce the group velocity dispersion curve  $v_g(\omega)$  from  $v_\varphi(\omega)$ , as  
 253 these two quantities are linked in elastic mediums by the following relation [29] :

$$v_\varphi = \frac{\omega}{k} \quad \text{and} \quad v_g = \frac{\partial \omega}{\partial k} \quad (3)$$

254 However, in the case of experimental measurements, the numerical derivation of  $v_\varphi(\omega)$  is per-  
 255 turbed by the quick small fluctuations in measured values. Using another processing method to  
 256 evaluate the coherent group velocity from the measurements provide additional complementary  
 257 information on the propagation.

258  $v_g(\omega)$  provides information about the velocity of wave-packets centered around a given fre-  
 259 quency. It is classically obtained by the calculation of spectrograms, or through the Multiple  
 260 Filter Analysis (MFA) [30]. The principle is the following: the signal is filtered in the frequency  
 261 domain by a series of narrow Gaussian filters centered around various frequencies  $f_i$ . The width  
 262 of each filter  $i$  is chosen at  $\Delta f_i = 0.7f_i$ . Each filtered signal produces a wave-packet in the time  
 263 domain. It is then possible to draw a time-frequency representation of the signals. The time  
 264 of flight  $\Delta t_i$  of the maximum of the envelope of each wave-packets is then evaluated between  
 265 two acquisition points separated by a distance  $\Delta d$ , providing an evaluation of the group velocity  
 266 around the frequency  $f_i$ .

267 This method lead to systematic errors as with many time-frequency representations. Kodera  
 268 *et al* [31] present a method called reassignment to improve the accuracy of time-frequency rep-  
 269 resentations, using the fact that these kind of errors are predictable if the filters are known. This  
 270 notion was later developed in a practical way and generalised by Auger and Flandrin [32]. Clas-  
 271 sical time frequency methods such as MFA allocate the energy of the signal at a point in the  
 272 time-frequency plane. Due to the width of the filters used, at a given frequency the energy is  
 273 spread around its real location. The principle is to change the attribution point of this energy  
 274 and to assign it to the center of gravity of all these energy contributions. Then the reassignment  
 275 method improves the sharpness of the localisation of the signal components by reallocating its  
 276 energy distribution in the time-frequency plane. The efficiency of this method applied on sur-  
 277 face waves was presented by Pedersen [33]. The development of the method is fully presented  
 278 in [32, 33] and is over the goal of this paper.

279 Only two reception points are theoretically needed to compute the reassigned MFA maps. As  
 280 we use an array of 36 reception points, it is possible to produce a variety of time-frequency maps.

281 We choose to take the first reception point at  $d_1$  as a reference and then compute reassigned MFA  
 282 maps with the signals from reception points number 10 ( $d_{10} - d_1 = 9$  cm) to the number 30  
 283 ( $d_{30} - d_1 = 29$  cm) and then compute the average of the maps. Reception signals acquired too  
 284 close to the reference signal are not used as too small  $\Delta d$  and  $\Delta t_i$  induce great fluctuations in the  
 285 result. The farthest reception points do not contain enough energy compared to the noise level  
 286 and are also eliminated. The coherent  $v_g(\omega)$  is then picked from the maxima of this average map.

### 287 5.3. Attenuation factor

288 The attenuation factor is estimated from the decrease of the amplitude spectrum of the coher-  
 289 ent field during propagation.

290 In the frequency domain, the amplitude  $A(\omega, d_i)$  in equation (1)-(2) is assumed to take the  
 291 following expression (Eq. 4):

$$A(\omega, d_i) = A_1(\omega)e^{-\alpha(\omega)(d_i-d_1)}, \quad (4)$$

292 where  $A_1(\omega)$  is the amplitude of  $s$  at the first receiver located at the offset  $d_1$ . The attenuation  
 293 parameter  $\alpha(\omega)$  is determined by the slope of a least-square linear fit of  $\ln(A(\omega, d_i))$ . To elimi-  
 294 nate small noise variation in the spectrums, a light smoothing was performed on each coherent  
 295 amplitude spectrums with a moving average over  $f$ . Geometrical spreading was corrected by  
 296 multiplying the signals by  $\sqrt{d_i}$  (see Sec. 4.1).

297 In the same way as for the phase velocity, the attenuation factor for lower frequencies will be  
 298 estimated using the whole reception points of the setup (36 reception points), while for the higher  
 299 frequencies only the first reception points containing enough energy will be used, according to  
 300 the study of Sec. 4.2.

## 301 6. Results and discussion

### 302 6.1. Phase velocity

303 Experimental coherent phase velocity dispersion curves are presented in Fig. 9. The two  
 304 concretes are represented with the empty circle and triangles, while the mortars are presented  
 305 with the filled items. Series with the same item share the same  $w/c$  ratio; triangles correspond to  
 306  $w/c = 0.65$  and circles correspond to  $w/c = 0.35$ .

307 The curves are clearly distinguishable the one from the other. For a given  $w/c$  ratio of the  
 308 cement paste, the presence of the aggregates increases the phase velocity of about 10%. The fact  
 309 that the phase velocity also decreases with the increase of  $w/c$  is commonly observed [9], as a  
 310 high  $w/c$  ratio induces higher porosity and hence lower mechanical strength.

311 For the series with the higher  $w/c$  ratio (B2 and M2), a slight decrease can be noticed on  
 312 the dispersion curves of the phase velocity. This decrease can also be noticed on concrete B1,  
 313 but is less important. For Rayleigh waves, this is in general due to a gradient of properties of  
 314 the material with depth; larger wavelengths penetrate deeper whereas short wavelengths are only  
 315 sensitive to the upper part of the material, leading to different phase velocity values if a gradient  
 316 is present. It is known that aggregate distribution with depth is non uniform due to wall effects, as  
 317 the bigger aggregates cannot be as close to the surface as half their dimension [34]. However, as  
 318 this phenomenon occurs either on concrete B2 or mortar M2, containing only small particles, this  
 319 aggregate distribution effect is not the main cause of this dispersion behaviour. A change of free  
 320 water content may be envisaged, due to a drying of the surface of the slabs during the experiment,  
 321 but weight measurements showed that the water loss was negligible. It is also remarkable that

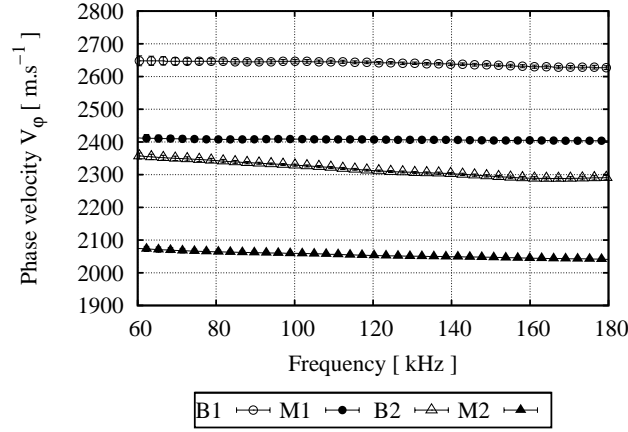


Figure 9: Dispersion curves for the coherent phase velocity  $v_\varphi(\omega)$ .

322 this decrease is less important in the case of low  $w/c$ , with low porosity. Then the reason of the  
 323 dispersive behaviour for M2 and B2 can be a change of porosity with depth.

324 6.2. Group velocity

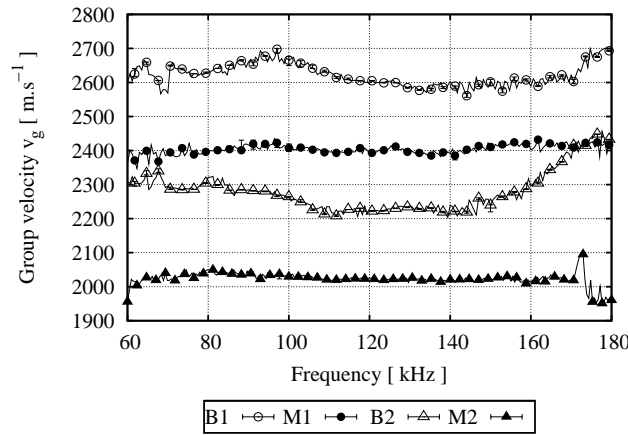


Figure 10: Dispersion curves for the coherent group velocity  $v_g(\omega)$ .

325 Coherent group velocities dispersion curves show additional information about the propaga-  
 326 tion of waves. For non-dispersive materials, group and phase velocities should be equal, but their  
 327 values differ in dispersive media. Experimental results (Fig. 10) show some similarities with the  
 328 phase velocity dispersion curves (Fig. 9). The 4 series are clearly distinguishable the one from  
 329 the others, and the average group velocity is close to the average phase velocity.

330 The main difference is the behaviour of the two concrete series B1 and B2. While the mortar  
 331 series M1 and M2 show a nearly constant group velocity, both concrete series show similar varia-  
 332 tions with frequency. Group velocity decreases around 100 kHz of about  $100 \text{ m.s}^{-1}$ , stabilises,

333 and increases again after 150 kHz. B1 and B2 containing the same amount, nature and size of ag-  
 334 gregates, the presence of the aggregates clearly modifies the coherent group velocity dispersion  
 335 of Rayleigh waves.

336 In this frequency range, the presence of aggregates is more clearly visible on the coherent  
 337 group velocity dispersion curves than on the coherent phase velocity, as  $v_g(\omega)$  shows a particular  
 338 signature when aggregates are present. On the contrary, a change in the  $w/c$  ratio is more visible  
 339 on the coherent phase velocity measurements by the dispersion of  $v_\varphi(\omega)$ . These two coherent  
 340 velocity measurements provide complementary information on the concrete or mortar. It is then  
 341 important to make a distinction between phase and group velocity measurements to characterise  
 342 concrete as their sensitivity are different in this frequency range.

### 343 6.3. Attenuation factor

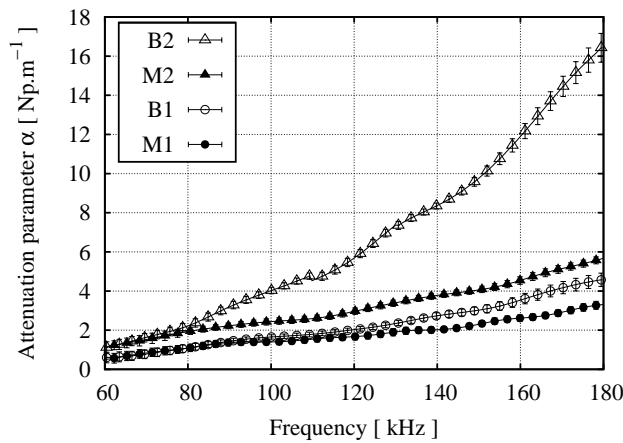


Figure 11: Coherent attenuation parameter  $\alpha(\omega)$ .

344 Attenuation parameter measurements are of great interest in non-destructive evaluation, as  
 345 attenuation is sensitive both to microstructural and viscoelastic parameters of the media. How-  
 346 ever, interpretation is complex because the attenuation parameter measured (i.e. the decrease  
 347 of the frequency component with the distance of propagation) contains information about all  
 348 the attenuative processes : geometrical spreading, scattering by large and small heterogeneities  
 349 (aggregates, sand, air voids, pores,...), and intrinsic attenuation due to the viscoelasticity of  
 350 the materials. All these effects are mixed together and it is difficult to evaluate the contribu-  
 351 tion of a single effect. Geometrical spreading effects were corrected in Sec.4.1. Thus, coherent  
 352 attenuation parameter curves presented in Fig. 11 contain information about the scattering by  
 353 aggregates, attenuation due to porosity and micro-cracks of the cement paste, and attenuation  
 354 due to viscoelasticity.

355 For the mortar series M1 and M2, the attenuation factor curves are almost linear with fre-  
 356 quency, and a higher  $w/c$  (higher porosity) logically induces a higher values of the attenuation  
 357 parameter. When aggregates are present, the effect of scattering by the aggregates are added to  
 358 the other effects. The contribution of the multiple scattering can be deduced by comparing the  
 359 mortar and concrete sharing the same  $w/c$  and mix properties (B1-M1 or B2-M2).

360 At low frequencies, no difference is visible between a concrete and its corresponding mortar  
 361 (below 80 kHz for B1-M1, and below 120 kHz for B2-M2), the effect of the aggregates is  
 362 negligible comparing to all other effects. As the frequency increases, the wavelength becomes  
 363 comparable with the aggregate size, and the attenuation parameter increases due to scattering.  
 364 For  $w/c = 0.35$  (B1-M1), these scattering effects are not important, and the attenuation parameter  
 365 increases only of about  $1 \text{ Np.m}^{-1}$ . On the contrary, for  $w/c = 0.65$ , the change in the  
 366 attenuation factor due to aggregates is very important. It is difficult to distinguish the three series  
 367 B1, M1 and M2, while B2 is clearly different.

368 Concretes series B1 and B2 share the same kind and quantity of aggregates, and differ only  
 369 by their  $w/c$ . Multiple scattering does not only depend on the shape and size of the scatterers,  
 370 but also on the contrast between the mortar and the aggregates. For various  $w/c$  the macroscopic  
 371 properties of mortar are different what can explain the change of attenuation. Moreover, when  
 372 porosity of the cement paste is high, contact between aggregates and mortar may be non perfect,  
 373 this modification of the microstructure in the interface zone may cause the distinct behaviour of  
 374 the attenuation curves. This investigation can not distinguish between these two hypotheses, but  
 375 highlight that evaluation of attenuation of wave in concrete looks very efficient to evaluate and  
 376 characterise concrete.

### 377 7. Configurations of disorder

378 Coherent phase velocity, group velocity, and coherent attenuation parameter studied in the  
 379 section before were measured using a voluntarily high number of configuration of disorder  $N_{dis}$   
 380 for the evaluation of the coherent field :  $N_{dis} = 90$  for the concrete series and  $N_{dis} = 36$  for  
 381 the mortar series. As a result, the evaluation of the coherent propagation parameters are very  
 382 accurate and correctly take into account the heterogeneous nature of the materials. In particular,  
 383 coherent attenuation parameters measurements show that the difference between B1, M1 and M2  
 384 is very low (less than  $2 \text{ Np.m}^{-1}$ ), but all three series can still be compared due to the accuracy of  
 385 the measurements. However, it is usually not possible to acquire 90 different configurations of  
 386 disorder, for economic or time reason. Fig. 12 and 13 show the influence of  $N_{dis}$  on the value of  
 387 the phase velocity and the attenuation factor at low frequencies (60 kHz) and high frequencies  
 388 (180 kHz).

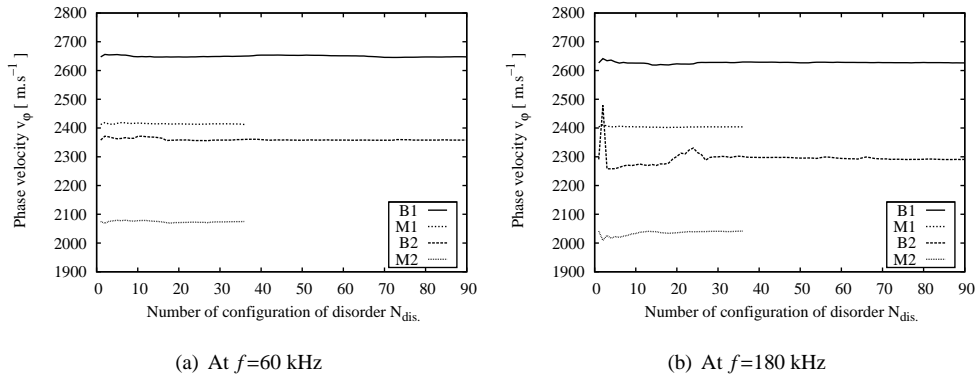


Figure 12: Influence of the number of configurations of disorder on the evaluation of the phase velocity  $v_\phi$ .

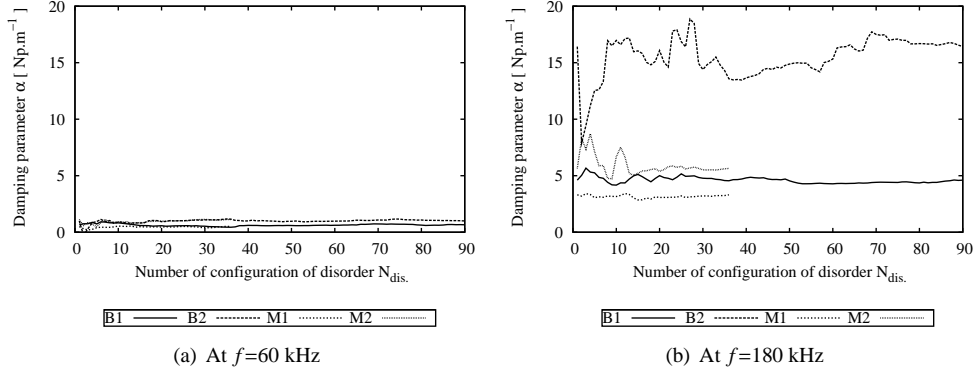


Figure 13: Influence of the number of configurations of disorder on the evaluation of the attenuation parameter  $\alpha$ .

389 Both  $v_\varphi$  and  $\alpha$  present fluctuations as the number of configurations of disorder increases,  
 390 and comes to a stabilisation. The number of configurations required to get to this stabilisation  
 391 depends strongly with the frequency : for low frequency, the values of  $v_\varphi$  and  $\alpha$  stabilise quickly,  
 392 while a relatively high value of  $N_{dis}$  is needed to reach a complete stabilisation at 180 kHz.

	B1	M1	B2	M2
$N_{opt.}$ for $v_\varphi$	20	1	30	10
$N_{opt.}$ for $\alpha$	50	5	70	15

Table 2: Optimal number of configurations of disorder required to get stabilisation of the attenuation parameter  $\alpha$  with  $N_{dis}$  at  $f = 180$  kHz.

393 The value of  $\alpha$  is much more sensitive to  $N_{dis}$  than  $v_\varphi$ , because the relative amplitude of  
 394 the fluctuation of  $\alpha$  is important compared to the stabilised value. Table 2 shows the optimal  
 395 number of independent configurations of disorder  $N_{opt.}$  required to get a stable value of  $\alpha$  (at  
 396  $\pm 0.5$  Np.m<sup>-1</sup>) or  $v_\varphi$  (at  $\pm 10$  m.s<sup>-1</sup>) at the frequency  $f = 180$  kHz. It is clear that the evaluation  
 397 of coherent  $v_\varphi$  requires less configurations of disorder than the evaluation of  $\alpha$ . These values  
 398 of  $N_{opt.}$  can be directly linked with the degree of heterogeneity of the material at the frequency  
 399 considered. In particular, concrete series need more configurations of disorder than mortar and  
 400 an increase of  $w/c$  increases the  $N_{opt.}$  required. If the value of  $N_{dis}$  chosen for the measure-  
 401 ments is too low, the coherent field will not be properly evaluated and the error on  $\alpha$  or  $v_\varphi$  will  
 402 increase; comparison between two series with very similar propagation parameters (for example  
 403 comparing the attenuation parameter  $\alpha$  for B1 and M1) will not be possible.

## 404 8. Concluding remarks

405 Surface waves are well adapted to characterise cover concrete. Coherent phase velocity,  
 406 group velocity and attenuation parameter show sensitivities to different properties of concrete:  
 407  $w/c$  ratio, presence of aggregates, ... The accuracy of the estimations of the propagation param-  
 408 eters  $v_\varphi$ ,  $v_g$  and  $\alpha$  is primordial to characterise properly the materials, as many phenomena are  
 409 involved in the propagation of Rayleigh waves in concrete.

410 Geophysical methods provide appropriate signal processing tools for the treatment of Rayleigh  
411 waves. Particular attention has to be drawn to the acquisition setup required by these signal pro-  
412 cessing tools. Another key point is the use of coherent waves, obtained by averaging the signals  
413 over a large amount of configurations of disorder. Propagation parameters of the coherent waves  
414 provide information on the mean mechanical properties of the concrete, avoiding effects due to  
415 a particular configuration of the concrete that are non representative of the average structure.

416 The experimental procedure presented in this paper has proved to be very efficient to under-  
417 line differences between different concrete and mortar samples. However these differences come  
418 from different phenomena coupled together. Then a better understanding of the propagation of  
419 Rayleigh waves in such complex media is needed, to be able to evaluate mechanical parameters  
420 such as Young modulus, Poisson ratio, or porosity. In particular, a model of the multiple scattering  
421 process by the heterogeneities have to be studied to distinguish the attenuation process due  
422 to scattering and the one due to porosity or viscoelasticity [35]. Dispersion of the coherent phase  
423 and group velocity of Rayleigh waves can be used to estimate variations of properties with depth.  
424 This approach is commonly used in geophysics [36].

425 Subsequently, the case of damaged concrete, for example carbonation, cracks or micro-  
426 cracks, have to be studied to show the ability of our method to detect and identify some defaults.  
427 Furthermore, a special robot equipped with a smaller laser interferometer is being developed to  
428 be used *in situ* on real concretes structures.

## 429 Acknowledgements

430 This study was funded in part by the French National Research Agency (ANR ACTENA,  
431 ANR SEISCOPE) and the French Region "Pays de la Loire". The authors wish to thank grate-  
432 fully the TGCE department of the LCPC, who designed the mix proportions of the concretes and  
433 prepared the slabs.

## 434 References

- 435 [1] P.E Grattan Bellew, "Microstructural investigation of deteriorated Portland cement concretes", *Construct. Build.*  
436 *Mat.* 10(1), pp. 3-16 (1996)
- 437 [2] V.M. Malhotra, N.J. Carino, "Handbook on nondestructive testing of concrete", CRC Press LLC, (1991)
- 438 [3] M.F. Kaplan, "The effects of age and water to cement ratio upon the relation between ultrasonic pulse velocity and  
439 compressive strength of concrete", *Mag. Concr. Res.* 11(32), pp. 85 (1959)
- 440 [4] F.P. Zhou, F.D. Lydon and B.I.G. Barr, "Effect of coarse aggregate on elastic modulus and compressive strength of  
441 high performance concrete", *Cem. Concr. Res.* 25(1), pp. 177-186 (1995)
- 442 [5] W. Punurai, J. Jarzynski, J. Qu, K.E. Kurtis and L.J. Jacobs, "Characterisation of entrained air voids in cement paste  
443 with scattered ultrasound", *NDT&E Int.* 39, pp. 514-524 (2006)
- 444 [6] D.G. Aggelis, D. Polyzos and T.P. Philippidis, "Wave dispersion and attenuation in fresh mortar: theoretical predic-  
445 tions vs. experimental results", *J. Mech. Phys. Solids* 53, pp. 857-883 (2005)
- 446 [7] J.F. Chaix, V. Garnier and G. Corneloup, "Ultrasonic wave propagation in heterogeneous solid media: Theoretical  
447 analysis and experimental validation", *Ultrasonics* 44, pp. 200-210 (2006)
- 448 [8] E.N. Landis and S.P. Shah, "Frequency-Dependent Stress Wave Attenuation in Cement-Based Materials", *J. Eng.*  
449 *Mech. - ASCE* 121 (6), pp. 737-743 (1995)
- 450 [9] T.P. Philippidis and D.G. Aggelis, "Experimental study of waves dispersion and attenuation in concrete", *Ultrason-*  
451 *ics*, 43, pp. 584-595 (2005).
- 452 [10] L. Qixian and J.H. Bungey, "Using compression wave ultrasonic transducers to measure the velocity of surface  
453 waves and hence determine dynamic modulus of elasticity for concrete", *Constr. Build. Mater.* 10(4) pp. 237-242  
454 (1996)
- 455 [11] S. Ould-Naffa, M. Goueygou, B. Piwakowski and F. Buyle-Bodin, "Detection of chemical damage in concrete  
456 using ultrasound", *Ultrasonics* 40, pp. 247-251 (2002)

- 457 [12] G. Villain, X. Derobert, O. Abraham, O. Coffec, O. Durand, L. Laguerre and V. Baltazart, "Use of ultrasonic  
458 and electromagnetic NDT to evaluate durability monitoring parameters of concrete", *Proceedings of Non Destructive*  
459 *Testing on Civil Engineering Conference NDTCE'09, Nantes, France* (2009)
- 460 [13] B. Piwakowski, A. Frine, M. Goueygou and F. Buyle-Bodin, "Generation of Rayleigh waves into mortar and  
461 concrete samples", *Ultrasonics* 42, pp. 395-402 (2004)
- 462 [14] L.J. Jacobs and R.W. Whitcomb, "Laser generation and detection of ultrasound in concrete", *J. Nondestructive*  
463 *Evaluation* 16, pp. 57-65 (1997)
- 464 [15] J.O. Owino and L.J. Jacobs, "Attenuation Measurements In Cement-Based Materials Using Laser Ultrasonics", *J.*  
465 *Eng. Mech. - ASCE* 125 (6), pp. 637-647 (1999)
- 466 [16] L.J. Jacobs and J.O. Owino, "Effect of Aggregate Size on Attenuation of Rayleigh Surface Waves in Cement-Based  
467 Materials", *J. Eng. Mech. - ASCE* 126 (11), pp. 1124-1130 (2000)
- 468 [17] D.G. Aggelis and T. Shiotani, "Experimental study of surface wave propagation in strongly heterogeneous media",  
469 *J. Acoust. Soc. Am* EL 122(5) EL151-EL157 (2007)
- 470 [18] D.G. Aggelis and T. Shiotani, "Surface wave dispersion in cement-based media: Inclusion size effect", *NDT&E*  
471 *Int.* 41, pp. 319-325 (2008)
- 472 [19] N. Krstulovic-Opara, R.D. Woods and N. Al-Shayea, "Nondestructive testing of concrete structures using the  
473 Rayleigh wave dispersion method" *ACI Mater. J.* pp. 75-86 January-February (1996)
- 474 [20] J. Lagarde, O. Abraham, L. Laguerre, P. Côte, J.P. Piguet, C. Balland and G. Armand, "Use of surface waves and  
475 seismic refraction for the inspection of circular concrete structures", *Cem. Concr Compos.* 28, pp. 337-348 (2006)
- 476 [21] A. Derode, A. Tourin and M. Fink, "Random multiple scattering of ultrasound. I. Coherent and ballistic waves",  
477 *Phys. Rev. E* 64 (2001)
- 478 [22] L.L. Foldy, "The multiple scattering of waves", *Phys. Rev.* 67(3-4), pp. 107-119 (1945)
- 479 [23] P. Anugonda, J.S. Whien and J.A. Turner, "Diffusion of ultrasound in concrete", *Ultrasonics*, 39, pp. 429-435  
480 (2001)
- 481 [24] S.K. Ramamoorthy, Y. Kane and J.A. Turner, "Ultrasound diffusion for crack depth determination in concrete", *J.*  
482 *Acoust. Soc. Am.*, 115(2), pp. 523-529 (2004)
- 483 [25] G.A. McMechan and M.J. Yedlin, "Analysis of dispersive waves by wave field transformation", *Geophysics* 46(6),  
484 pp. 869-874 (1981)
- 485 [26] T.A. Mokhtar, R.B. Herrmann and D.R. Russel, "Seismic velocity and Q model for the shallow structure of the  
486 Arabian shield from short-period Rayleigh waves", *Geophysics* 53(11), pp. 1379-1387 (1988)
- 487 [27] T. Forbriger, "Inversion of shallow-seismic wavefield: I. Wavefield transformation", *Geoph. J. Int.* 153, pp. 719-734  
488 (2003)
- 489 [28] R.B. Herrmann, "Computer Program in Seismology", *Department of Earth and Atmospheric Sciences*, Saint Louis  
490 University (2002)
- 491 [29] J.M. Carcione, "Wave fields in real media : wave propagation in anisotropic, anelastic and porous media", in  
492 *Handbook of Geophysical Exploration*, edited by K. Helbig and S. Treitel (2001)
- 493 [30] A. Dziewonsky, S. Bloch and N. Landisman, "A technique for the analysis of transient seismic waves" *Bull. Seis.*  
494 *Soc. Am.* 59, pp. 427-444 (1969)
- 495 [31] K. Kodera, C. De Velledary and R. Gendrin, "A new method for the numerical analysis of nonstationary signals",  
496 *Phys. Earth. Planet. Internat.* 12, pp. 142-150 (1976)
- 497 [32] F. Auger and P. Flandrin, "Improving the readability of time frequency and time-scale representation by the reas-  
498 signment method", *IEEE Trans. Sig. Proc.*, 43(5), 1068-1089 (1995)
- 499 [33] H.A. Pedersen, J.I. Mars and P. Amblard, "Improving surface-wave group velocity measurements by energy reas-  
500 signment". *Geophysics*, 68(2), pp. 677-684 (2003)
- 501 [34] J.J. Zheng, C.Q. Li and M.R. Jones, "Aggregate distribution in concrete with wall effect", *Mag. Concr. Res.* 55(3),  
502 pp. 257-265 (2003)
- 503 [35] M. Chekroun, L. Le Marrec, B. Lombard, J. Piroux and O. Abraham, "Comparison between a multiple scattering  
504 method and direct numerical simulation for elastic wave propagation in concrete", *Springer Ser. wave Phenomena*  
505 (2008) accepted for publication.
- 506 [36] L. Bodet, K. Van Wijk, A. Bitri, O. Abraham, P. Cte, G. Grandjean and D. Leparoux, "Surface-wave inversion  
507 limitations from laser-Doppler physical modeling", *J. Env. and Eng. Geophys.* 10(2), pp . 13-24 (2005)